Review

Peripheral nerve stimulation by induced electric currents: exposure to time-varying magnetic fields

J. P. Reilly

The Johns Hopkins University, Applied Physics Laboratory,
Johns Hopkins Road, Laurel, MD 20707-6099, USA

Abstract—*The review evaluates thresholds of peripheral nerve stimulation by complex current waveforms. A neuroelectric model employing Frankenhaeuser-Huxley membrane nonlinearities is used to derive excitation thresholds for monophasic and biphasic pulse sequences, as well as sinusoidal stimuli. The model, along with principles of magnetic field induction, is used to derive criteria of acceptability for exposure to time-varying magnetic fields. Applications to pulsed gradient fields from magnetic resonance imaging devices are discussed.*

Keywords—*Electric shock, Electrical safety, Electrical stimulation, Magnetic field exposure, Magnetic resonance imaging, Neural excitation*

Med. & Biol. Eng. & Comput., 1989, **27**, 101–110

1 Introduction

A PERSON exposed to electric currents may experience a number of undesirable reactions whose severities depend on a host of factors, including stimulus magnitude, waveshape, repetition pattern and current distribution in the body. Undesirable effects of short-term exposure may include unpleasant or painful sensations, involuntary muscle contractions, burns, cardiac arrythmias and cardiac fibrillation. Industry and regulatory groups have sought to understand the biological effects of electric currents so that criteria could be developed to limit hazardous exposures through equipment safeguards or other precautionary measures.

In the past, guidelines regarding acceptability of short-term electrical exposure have been developed mainly for sinusoidal currents, and at power frequencies. Historically, the need for such criteria has been prompted by the widespread use of AC electic power. Criteria for power-frequency exposure acceptability have made use of human and animal data regarding sensory thresholds, muscle tetanus and ventricular fibrillation from sinusoidal currents (DALZIEL, 1972). More recently, perception and pain thresholds have been determined for electrocutaneous stimulation by sinusoidal currents with frequencies up to 200 kHz (CHATTERJEE *et al.*, 1986), and for capacitive discharges and 60 Hz electric field induction stimuli (REILLY and LARKIN, 1987).

There are also instances in which people may be exposed to nonsinusoidal stimuli. Such exposures may not necessarily be accidental. Sometimes, electric currents may be deliberately introduced, or they may be an unavoidable byproduct of a particular device. To illustrate this point, consider the use of magnetic resonance imaging (MRI) devices. These devices require that the patient be exposed to time-varying magnetic fields. The applied fields induce in the body currents having complex waveform patterns. Although existing guidelines on MRI magnetic fields have been adequate to preclude any known biological problems to date, the MRI industry would like to have greater flexibility in developing future designs. Industry and regulators need a rational methodology with which to develop acceptability criteria for a variety of complex stimulus waveforms.

The purpose of this review is to present a rational methodology for evaluating excitation thresholds for peripheral nerves stimulated by induced pulsatile electric currents. One motivation for this work is the need to refine the methods for developing acceptability standards for exposure to pulsed gradient fields from MRI devices. The methods developed here should be equally applicable to other pulsed current exposures, whether induced by pulsed magnetic fields or by other means.

2 Time-varying magnetic field induction

In accordance with Faraday's law, the electric field $\boldsymbol{E}$ is related to the time rate of change of flux density $\boldsymbol{B}$ by

$$\oint \boldsymbol{E} \cdot \boldsymbol{dl} = \frac{d}{dt} \iint \boldsymbol{B} \cdot \boldsymbol{ds} \tag{1}$$

The first integral is taken over a closed path, and $\boldsymbol{ds}$ is the element of area normal to the direction of $\boldsymbol{B}$. Each term in the integrals is a vector quantity. Elsewhere in this review the symbols B and E are used to represent scalar quantities. If B is uniform over the region inside a closed path of radius r, the induced electric field strength calculated from eqn. 1 is

$$E = \frac{r}{2} \frac{dB}{dt} \tag{2}$$

where the direction of the field is along the circumference

First received 16th May and in final form 19th September 1988

of the circle. In some applications the magnetic field varies sinusoidally as $B = B_0 \sin 2\pi ft$, and eqn. 2 becomes

$$E = [r\pi f B_0] \cos 2\pi ft \quad (3)$$

where the term in brackets is the peak induced electric field during the sinusoidal cycle, and B_0 is the peak magnetic field.

For induction in a volume conductor, such as the human body, a simple treatment of the induction process treats the volume as if it were made up of concentric rings normal to the direction of B. As suggested by eqn. 2, the outermost rings would have the greatest electric field strengths. According to this simple model, the maximum electric field for whole-body exposure would be computed from eqn. 2, with r being the maximum circle radius that can be drawn on the body in a plane perpendicular to B. There are more sophisticated and accurate methods for determining induced fields within the body (SILNY, 1986); however, the simple method described here will suffice to illustrate the principles discussed in this review.

The current density resulting from the induced field is

$$J = E\sigma \quad (4)$$

where J is the current density in a direction aligned with E, and σ is the conductivity of the medium.

Gradient field waveforms currently used in MRI imaging typically consist of gated trapezoidal and sinusoidal waveforms as illustrated in Fig. 1*a*. Fig. 1*b* illustrates the associated *dB/dt* waveforms, which dictate the waveshape of the induced electric field and current density.

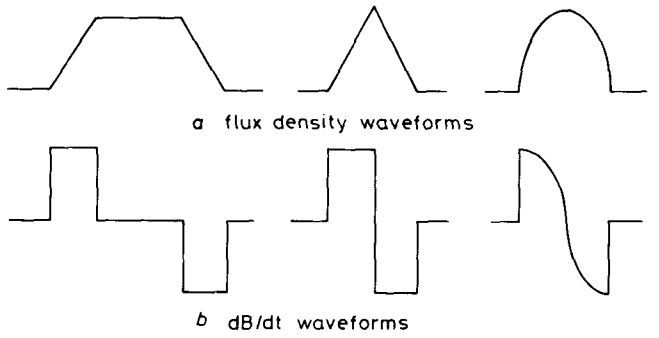

Fig. 1 *Example of flux density and dB/dt waveforms*

Typical pulse durations may be tenths to several milliseconds long. The field patterns may include sequences of pulses separated by intervals as short as several tenths of milliseconds and longer repetition patterns having periods some tens of milliseconds long. Considering the individual pulse waveshapes and repetition patterns, MRI induced currents can be quite complex.

An approach is needed to evaluate excitation thresholds for complex pulsatile waveforms. Most studies to date, however, apply to single monophasic rectangular pulses, or to continuous sinusoidal waveforms. Attempts have been made to generalise data from these studies to other stimulus waveforms using approaches based on linear Fourier analysis, linear network analysis or stimulus energy relationships. Such attempts are very limited in their applications because electrical properties of excitable tissue are markedly nonlinear. A rational approach for the evaluation of complex currents must account for the nonlinear response characteristics of excitable tissue.

3 Theoretical thresholds for neural excitation

3.1 *General properties*

A detailed description of the electrical properties of the excitable membrane was developed in the Nobel Prize-winning work by HODGKIN and HUXLEY (1952). They provided a detailed mathematical description of the electrical properties of the unmyelinated nerve membrane. This work was later extended by FRANKENHAEUSER and HUXLEY (1964), who provide a description of the myelinated nerve membrane. From these equations, one could study the complex inter-reactions between electric currents and the membrane properties. Myelinated fibres are distinguished from unmyelinated fibres by faster conduction rates, shorter action potential durations and lower electrical thresholds (RUCH *et al.*, 1968). Because of the lower thresholds, the myelinated fibre is a good choice for electrical stimulation studies.

A number of electrical cable type models have been developed incorporating the membrane equations to study stimulation by an intracellular electrode in an extended axon. One difficulty with intracellular stimulation models is that they are not readily adaptable to extracellular electrode placement, where the distribution of stimulus current along the fibre is an important factor. This difficulty was removed in the myelinated fibre model of MCNEAL (1976), who incorporated the Frankenhaeuser-Huxley membrane equations into an electrical array model to represent the interconnected nodes of a myelinated nerve. We have extended the McNeal format for more general applications, and refer to this modified representation as a spatially extended nonlinear node (SENN) model (REILLY *et al.*, 1985). The Appendix discusses the model in some detail, but limits the description to only those features needed to facilitate the present discussion. A more complete description of the model and its applications to electrical stimulation are provided in MCNEAL (1976), REILLY *et al.* (1985), REILLY and BAUER (1987) and REILLY (1988).

Fig. 2 illustrates two bipolar electrode arrangements for stimulating a nerve fibre. In Fig. 2*a* membrane current

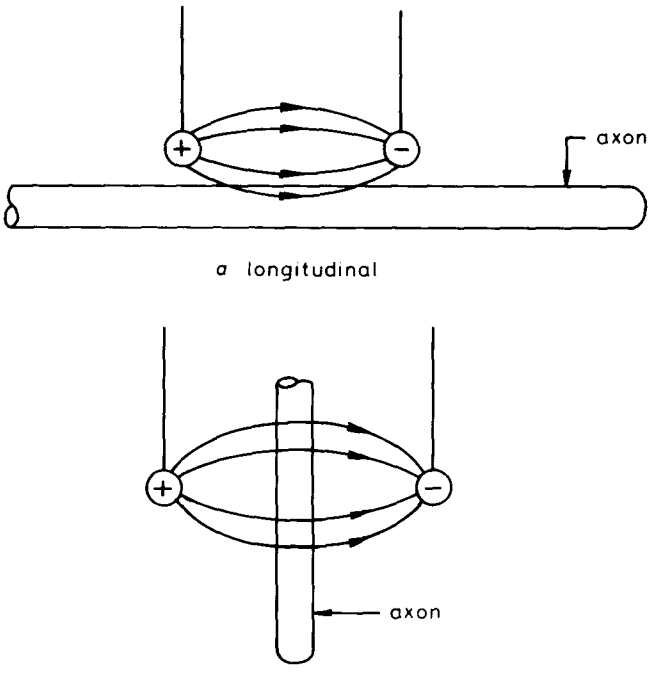

Fig. 2 *Longitudinal and transverse field excitation*

influx near the anode results in membrane hyperpolarisation in that region; current efflux near the cathode results in depolarisation. In Fig. 2*b* the membrane will be hyperpolarised on the side of the axon near the anode, and depolarised on the side near the cathode. A variety of

experimental studies have shown that the neuron is relatively insensitive to transverse field stimulation (as in Fig. 2*b*), relative to longitudinal stimulation (as in Fig. 2*a*, RANCK, 1975). Such experimental findings correspond to theoretical expectations (MCNEAL, 1976; MCNEAL and TEICHER, 1977).

In addition to a longitudinal orientation, the electric field must also have a spatial gradient to support excitation. This property can be appreciated with reference to eqn. 7 (Appendix), which shows that *second differences* of the external voltages appear as driving forces of the membrane potential. If the electric field were truly uniform, and the axon were infinite in both directions, there would in theory be zero net current transfer at every node. As a practical matter, however, the internal field is never uniform. Furthermore, an effective field gradient will be realised if the axon changes its spatial orientation with respect to a locally uniform field, or if the axon is terminated in the field, as with receptors, free nerve endings or nerve/muscle endplates.

Simulation results are presented in this review for uniform field excitation in which a uniform current density results in a constant voltage difference from node to node. In this mode, excitation is initiated at the terminus of the model axon.

Electrical thresholds are inversely related to fibre diameter, the large myelinated fibres having the lowest thresholds. For myelinated fibre diameters, the range is from about 2 to 22 μm (KANDEL and SCHWARTZ, 1981). Unmyelinated fibres have a range more typically from 0·3 to 1·3 μm. In this review SENN model thresholds are evaluated for fibre diameters of 5, 10 and 20 μm.

3.2 *Stimulation by monophasic currents*

Fig. 3 illustrates strength/direction (S/D) curves from the SENN model for single monophasic stimulus pulses in a uniform electric field. The vertical axes have been normalised to unity minimum value. The left vertical axis indicates the thresholds in units of the normalised electric field within the biological medium; the right-hand axis is in units of the product field × pulse duration. Alternatively, the threshold values can be expressed in terms of current density J or charge density q by multiplying the previously mentioned values by the conductivity of the medium.

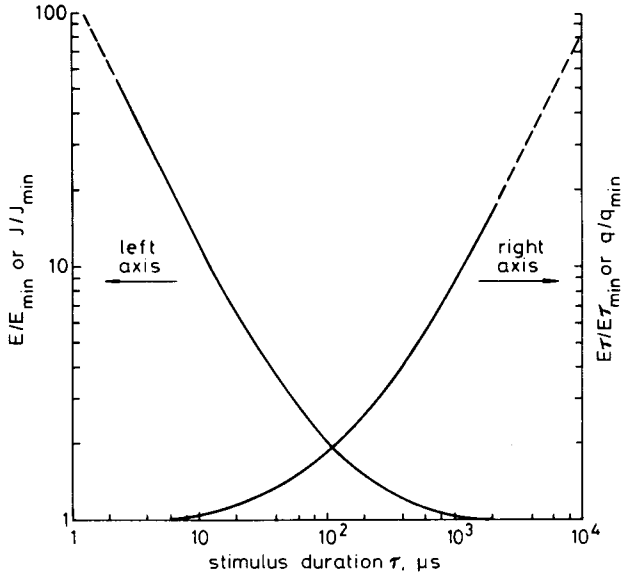

Fig. 3 *SENN model strength/duration curves for monophasic pulse stimulation in a uniform electric field. Units on the vertical axis have been divided by the minimum thresholds listed in Table 1*

Part (*a*) of Table 1 expresses the minimum threshold values used as normalising factors in Fig. 3. For long pulses ($\tau > 1$ ms), the minimum threshold is expressed in terms of the induced field. For short pulses ($\tau < 10$ μs), minimum threshold is given in terms of the product of field strength and pulse duration. Table 4 of the Appendix tabulates the data points used for Fig. 3.

Table 1 Minimum stimulus thresholds with uniform field excitation; single monophasic stimuli

Criteria	Fibre diameter, μm		
	5	10	20
(*a*) Field strength			
E_{min}, V m^{-1}	24·6	12·3	6·2
$E\tau_{min}$, V s m^{-1}	$2{\cdot}98 \times 10^{-3}$	$1{\cdot}49 \times 10^{-3}$	$0{\cdot}75 \times 10^{-3}$
(*b*) Current density			
J_{min}, A m^{-2}	4·92	2·46	1·23
q_{min}, C m^{-2}	$6{\cdot}0 \times 10^{-4}$	$3{\cdot}0 \times 10^{-4}$	$1{\cdot}5 \times 10^{-4}$

Notes: E_{min} and J_{min} apply to long pulses ($\tau \geq 1$ ms), $E\tau_{min}$ and q_{min} apply to short pulses ($\tau \leq 10$ μs). Current and charge density determined for conductivity $\sigma = 0{\cdot}2$ S m^{-1}

The longitudinal separation of nodes in a myelinated fibre is directly proportional to fibre diameter. Therefore, the absolute threshold in a uniform field is inversely proportional to fibre diameter. This can be seen with reference to eqn. 7: if the nodal separation is increased, the external nodal potential differences will increase proportionately. Table 1 expresses the SENN model minimum thresholds for fibre diameters of 5, 10 and 20 μm. These values effectively cover the diameter spectrum of myelinated fibres.

The electric field in the medium is the primary force governing stimulation. However, current density is perhaps a more frequently cited stimulation parameter. Part (*b*) of Table 1 expresses thresholds in units of current and charge density. These quantities are determined by multiplying E and $E\tau$ by the conductivity of the medium, σ. In Table 1, the quantities in part (*b*) were obtained from those in part (*a*) by assuming an example conductivity of $\sigma = 0{\cdot}2$ S m^{-1}. The values in part (*b*) are intended to facilitate comparison with other published data on current density thresholds. Comparisons with published current density thresholds would preferably include the actual conductivity applying to the particular experiment. Note, however, that the relevant stimulation force is the electric field in the biological medium, rather than current density *per se*.

3.3 *Biphasic stimuli*

The current reversal of a biphasic pulse can reverse a developing AP that was excited by the initial phase. To compensate for the reversal, a biphasic pulse may have higher threshold than a monophasic pulse. Fig. 4 illustrates threshold modifiers based on the SENN model for biphasic stimuli. The vertical axis interprets SENN model thresholds as multipliers M for a double pulse relative to the threshold for a single pulse of the same phase duration τ_p. The portion of the figure with $M > 1$ applies to a biphasic pulse doublet, where the current reversal has the same magnitude and duration as the initial pulse. The portion of the figure with $M < 1$ is for a monophasic pulse doublet. Fig. 4 applies if the initial pulse is cathodal. Stimulation is also possible with an initial anodal pulse, but the thresholds are elevated (REILLY *et al.*, 1985).

According to Fig. 4, biphasic threshold elevation depends on the pulse duration and the time delay for current reversal. Thresholds are most elevated when the pulse is short, and the current reversal immediately follows the initial pulse. If the phase reversal is delayed by 100 μs

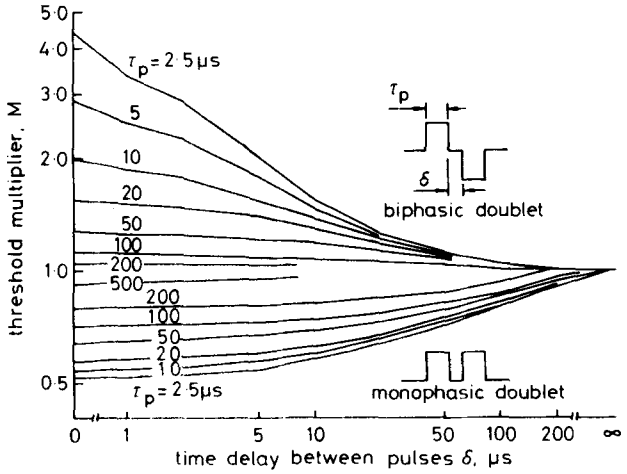

Fig. 4 *Threshold multipliers for biphasic and monophasic pulse doublets. The multiplier modifies the SENN model thresholds determined for a monophasic stimulus of duration τ_p, with uniform field excitation. The portion of the figure with $M > 1$ applies to a biphasic doublet; the portion with $M < 1$ applies to a monophasic doublet*

or more, there is little detectable effect on the biphasic pulse threshold.

The finding that thresholds are elevated for a single biphasic pulse should not be interpreted as implying that thresholds for all oscillatory stimuli are necessarily elevated above monophasic stimuli of the same phase duration. Indeed, if a biphasic stimulus is repeated as an oscillatory waveform, thresholds may decrease with successive oscillations to the point that they eventually fall below the single pulse monophasic threshold (see Section 3.5).

3.4 *Repetitive stimuli*

Repetitive stimuli can be more potent than a single stimulus through two mechanisms: threshold reduction from multiple pulse stimuli, and response enhancement due to multiple AP generation. In both cases there is an integration effect of the multiple pulses. In the first case, the integration takes place at the membrane level. In the second case, response enhancement takes place at the CNS level for neurosensory effects, and at the muscle level for neuromuscular effects.

Multiple pulse threshold effects are illustrated for two pulses in the lower section ($M < 1$) of Fig. 4. The figure gives the threshold multiple relative to a single pulse when there are two pulses of stimulation. The effects are most pronounced for short pulses and short interpulse delays. (In this representation, a delay of zero results in a single pulse of twice the duration.) Even at a delay of 200 μs, the integrative effects of a second pulse reduces the threshold by about 10 per cent for $\tau_p < 20$ μs. The SENN model was also exercised to evaluate the threshold modification for sequences of pulses numbering $N_p = 1$, 2, 4, 8, 16, 32, 64 and 128. Fig. 5 illustrates the results for several phase durations and interpulse delays. The vertical axis gives the threshold multiplier relative to a single pulse. The curve labelled $\delta = 0$ applies to continuous integration, and was determined from interpretation of Fig. 3. Threshold reduction due to pulse integration is increased as the pulse duration and delay time are shortened. At a delay of 500 μs, the SENN model shows no measureable pulse integration effect.

3.5 *Sinusoidal stimuli*

Acceptability standards for electric currents have traditionally been developed for sinusoidal stimuli. Considering the greater familiarity with such data, it is useful to relate thresholds for sinusoidal stimuli to the pulsatile stimuli.

Fig. 6 illustrates S/D curves from the SENN model for three types of stimuli: a monophasic rectangular waveform, a symmetric biphasic rectangular waveform, and a single cycle of a sine wave (from REILLY *et al.*, 1985). In this figure, excitation current is from a point electrode that is 2 mm radially distant from a 20 μm diameter fibre. The biphasic stimuli consist of a single stimulus cycle with an initial cathodal phase, followed by an anodal phase of the same magnitude and duration. The 'phase duration' indicated by the horizontal axis is that for the initial cathodal half-cycle. Stimulus magnitude is given in units of peak current on the left vertical axis, and in units of charge in a single monophasic phase on the right axis.

In Fig. 6, thresholds for the two biphasic waves at small values of τ_p are elevated above single monophasic thresholds because of the cancellation effect of current reversal

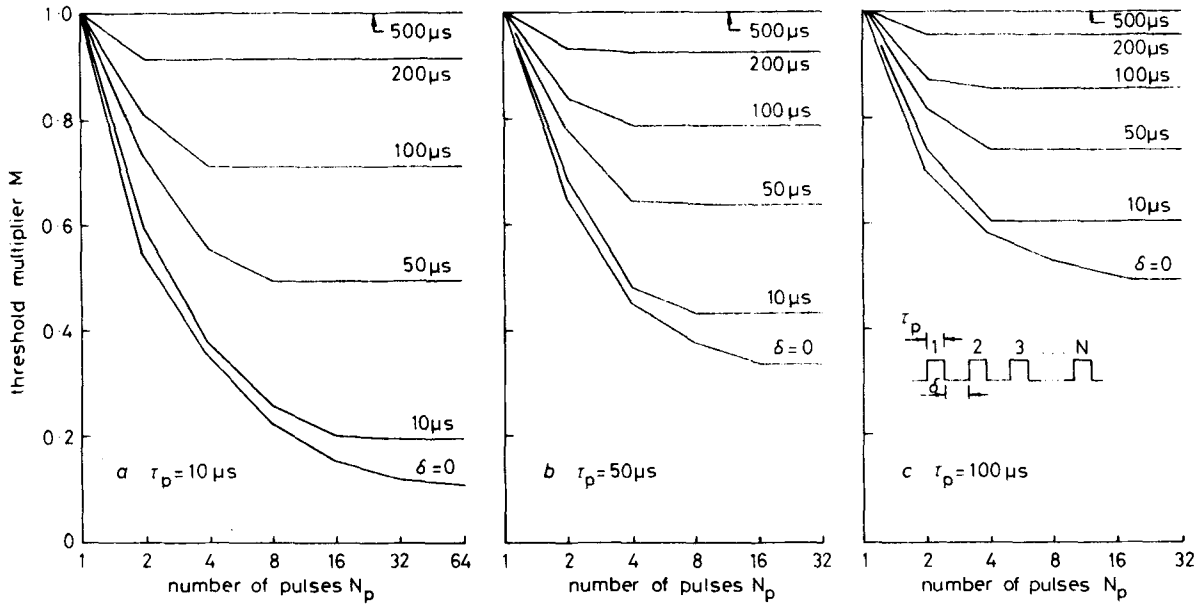

Fig. 5 *Threshold multipliers for repetitive pulse sequences — thresholds evaluated at $N_p = 1$, 2, 4, 8, 16, 32 and 64. Stimulation conditions as in Fig. 4*

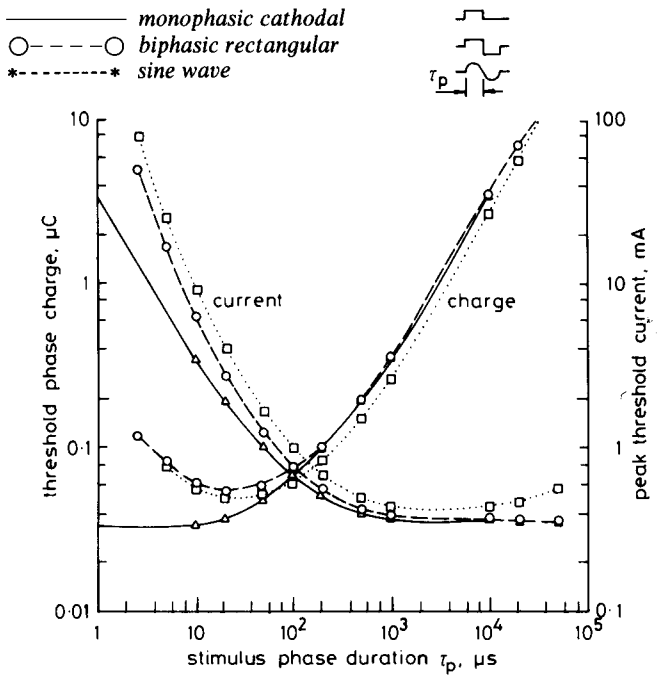

Fig. 6 *Strength/duration relationships derived from the SENN model: current thresholds and charge thresholds for single-pulse monophasic and for single-cycle biphasic stimuli with initial cathodal phases. Stimulation by point electrode 2 mm distant from 20 μm fibre. Threshold current refers to the peak of the stimulus waveform. Charge refers to a single phase for biphasic stimuli. (From* REILLY *et al., 1985)*

(discussed in Section 3.3). For long τ_p, this cancellation effect becomes ineffective, and thresholds depend more on the rate of rise and peak value of the current.

Fig. 7 illustrates the relationship between threshold and stimulus duration for sinusoidal waveforms having frequencies of 5 and 50 kHz (from REILLY *et al.*, 1985). When evaluated at half-cycle multiples, there is an oscillating threshold with minima at odd numbers of half-cycles, and maxima at even multiples. The full-cycle thresholds reach a minimum at eight cycles of stimulation with 5 kHz, and 64 cycles with 50 kHz. At a lower oscillation frequency rate of 500 Hz, thresholds were nearly independent of the number of stimulus cycles.

If a sinusoidal stimulus is at or near the threshold of a single cycle, a continuous repetition of cycles can generate multiple APs. This effect has been studied with the SENN model (REILLY *et al.*, 1985), showing that the AP repetition frequency increases with the sinusoidal amplitude and driving frequency. The maximum SENN model AP rate was about 500 Hz for stimulus levels 50 per cent above the single-cycle threshold. This rate is consistent with reported experimental neural properties of A-fibres, where the minimum interval between APs is about 2 ms for most practical cases (BRAZIER, 1977).

A comparison of SENN model results with experimental data is facilitated by strength/frequency (S/F) curves, a format that is often used for oscillating stimuli. Fig. 8 displays the results of Fig. 6 as a S/F relationship. The horizontal axis in Fig. 8 is the inverse of twice the phase duration in Fig. 6. Fig. 8 also shows a threshold curve for continuous sinusoidal stimulation based on the asymptotic values of Fig. 7.

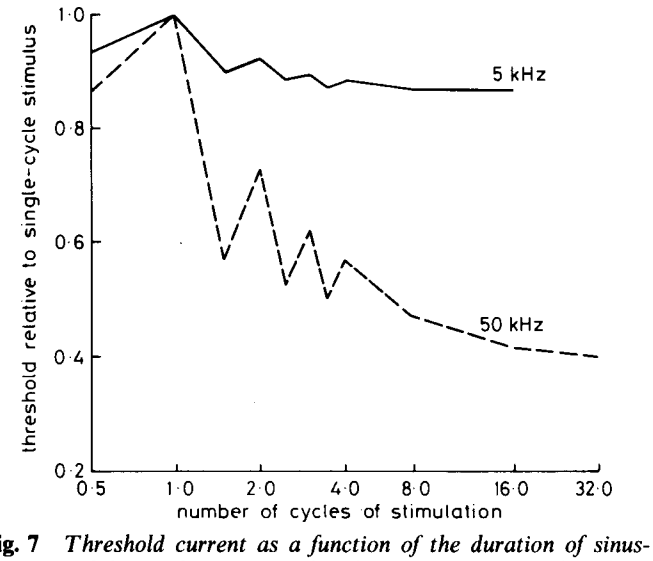

Fig. 7 *Threshold current as a function of the duration of sinusoidal stimulation. Stimulus duration was stepped in half-cycle increments out to four cycles, and in full-cycle increments beyond that point. Stimulation conditions as in Fig. 6. (From* REILLY *et al., 1985)*

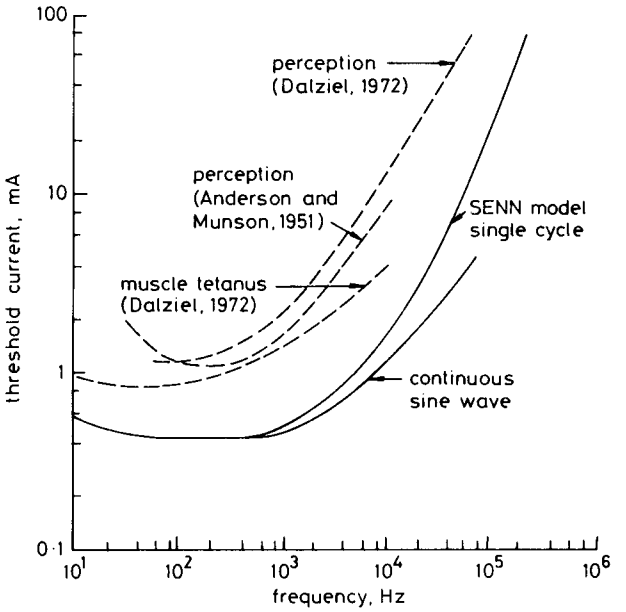

Fig. 8 *Strength/frequency curves for sinusoidal current stimuli. Broken curves are experimental data. Solid curves apply to the SENN model. Experimental curves have been shifted vertically to facilitate comparisons. Stimulation conditions as in Fig. 6. (Adapted from* REILLY *et al., 1985)*

Fig. 8 includes experimental threshold curves for human perception and muscle contraction (DALZIEL, 1972; ANDERSON and MUNSON, 1951). The experimental curves have been arbitrarily scaled on the vertical axis to facilitate comparison of the curve shapes; SENN threshold curves are plotted without adjustment. The shapes of the experimental and SENN curves correspond reasonably well considering that continuous stimulation was used in the cited experimental studies.

4 Experimental current density thresholds

Previous publications have compared SENN model thresholds with experimental data for a variety of monophasic and biphasic stimuli introduced through cutaneous or transcutaneous electrode systems. This section focuses on experimental thresholds that may be interpreted in relation to induced current density, and the determination of minimum excitation thresholds.

The simulation results presented in Fig. 3 and Table 1 apply to rectangular pulse current that produces a uniform electric field in the biological medium. Figs. 4–8 indicate additional relationships for other waveforms. For comparison purposes, it would be preferable to examine experimental data applying to similar conditions. Unfortunately,

Table 2 Experimental thresholds for neural stimulation

Item	Waveform of dB/dt or stimulus current	Duration ms	Subject/ preparation	Body locus	Response	Stimulus peak at threshold		Reference
						E, V m^{-1}	J, A m^2	
1	damped cosine, 3 kHz	2·0	rat	chest	twitch	34	5·1	McRobbie and Foster, 1984
2	¼ cycle cosine	0·083	rat	chest	twitch	45	6·8	"
3	½ cycle cosine	0·150	rat	chest	twitch	36	5·4	"
4	damped cosine, 3 kHz	2·0	human	forearm	sensation	25–50	3·8–7·5	"
5	damped cosine 2·1 kHz	*	human	forearm	EMG	78	11·8	"
6	¼ cycle cosine	0·12	human	forearm	EMG	113	16·7	"
7	½ cycle cosine	0·24	human	forearm	EMG	87	13·1	"
8	monophasic pulse	0·18	rat	whole body	muscle contraction	44–73	9–16*	Polson *et al.*, 1982*a*
9	monophasic pulse	0·18	human	wrist	EMG	70	14*	Polson *et al.*, 1982*b*
10	pulse*	2–3	frog nerve/ muscle		*	42–96	14–32	Ueno *et al.*, 1984
11	pulse*	2–3	frog nerve/ muscle		*	4·4	1·47	"
12	½ cycle cosine	2·0	frog nerve/ muscle		*	15	3·0*	Irwin *et al.*, 1970

* information sketchy or not available

available publications have not always provided a clear description of all the relevant details, such as a complete description of the stimulus waveform, its spatial orientation, the method of exposure, the biological preparation or subject, or the criterion for judging the presence of excitation. Nevertheless, available experimental data can be useful with some judgement and interpretation.

Table 2 summarises available experimental data (McRobbie and Foster, 1984; Polson *et al.*, 1982*a*; 1982*b*; Ueno *et al.*, 1984; Irwin *et al.*, 1970). Except for item 11, stimulation was via exposure to time-varying magnetic fields. With item 11, stimulation was via electrodes immersed in a saline bath. The two columns in Table 2 labelled 'stimulus peak at threshold' are of particular interest for our comparisons. In converting from field strength to current density, the value of conductivity cited in the reference was used. For items 8, 9 and 12, conductivity was not cited, so a value of 0·2 S m^{-1} was assumed. Except for item 11, stimulation current was induced by pulsed magnetic fields. For item 11, an electric field was created between metallic electrodes within the conducting medium.

The thresholds listed in Table 2 are not necessarily the minimum possible values, because the stimulus waveforms or field orientations were not necessarily optimum. As a result, a number of the listed thresholds should be reduced to obtain minimum possible values. Some specific comments on this point are as follows:

Items 1, 4 and 5. The *dB/dt* waveforms were damped cosine waves at 3·0 kHz. The sinusoidal stimulus threshold at 3 kHz is about a factor of 2 above that for the frequency region of greatest sensitivity between 50 and 500 Hz (Fig. 8).

Items 2 and 6. The *dB/dt* waveforms approximated a linear decay from a peak. The threshold level of a rectangular wave of the same duration can be as much as a factor of 2 below that for a triangular wave.

Items 3 and 7. The half-cycle cosine wave is biphasic. A rectangular biphasic wave with 75 μs phases would be reduced in sensitivity by about 20 per cent relative to a monophasic wave of 75 μs duration (Fig. 4). Additionally, the peak threshold of a cosine wave is greater than that for a rectangular wave of the same phase duration (Fig. 6).

Items 8 and 9. The threshold for a 180 μs pulse will exceed the minimum threshold for a long (1 ms) pulse by a factor of about 1·5 (Fig. 3).

Items 10 and 11. Details of the *dB/dt* waveshape were not provided. The direction of the field in item 10 was transverse to the nerve/muscle orientation. As noted in Section 3.1, this is an inefficient orientation for stimulation. In item 11, the preparation was placed in a saline bath, and the stimulus current was applied to electrodes within the bath. The orientation of the preparation relative to the field was not stated. Judging from the fact that the threshold was about one-tenth that in item 10, a transverse field orientation is suspected in item 11.

With consideration of the qualifications discussed above, the thresholds for items 1–10 might reasonably be reduced by a factor of 2 to obtain minimum thresholds for comparison with rectangular monophasic stimuli. This adjustment would bring the experimental values within the range of minimum theoretical thresholds listed in Table 1.

The data summarised in Table 2 exclude references to experiments in which current was introduced through electrodes held against the skin. One may be tempted to calculate electrocutaneous current density thresholds by dividing threshold current by contact area. Thresholds determined this way, however, may provide very conservative estimates of actual current density because current density beneath a contact electrode is concentrated at the edges of the electrode (Caruso *et al.*, 1979). Furthermore, with cutaneous electrodes, current is preferentially conducted in discrete cutaneous channels (Saunders, 1974).

5 Magnetic field exposure criteria

Thresholds of peripheral stimulation from magnetic field exposure may be developed from the principles discussed in Sections 2 and 3. The stimulation threshold of *dB/dt* can be expressed from eqn. 2 as

$$(dB/dt)_t = 2E_t/r \tag{5}$$

where E_t is the threshold electric field amplitude for a pulse of stimulus duration τ. For a conservative analysis, assume $r = 0{\cdot}2$ m, which would represent the largest circle radius that might be inscribed on the thorax or hips of a large person.

In accordance with Fig. 3, E_t for a rectangular mono-

phasic stimulus achieves a minimum value E_{min} when the pulse duration is long (> 1 ms). Table 3 summarises

Table 3 Flux density criteria for uniform field excitation; single monophasic stimuli

Criteria	Fibre diameter, μm		
	5	10	20
Flux density $(dB/dt)_{min}$, $T s^{-1}$	246	123	62
B_{min}, mT	30	15	7·5

Notes: Assumed loop radius: 20 cm
$(dB/dt)_{min}$ data apply to long pulses ($\tau \geqslant 1$ ms)
B_{min} data apply to short pulses ($\tau \leqslant 10\,\mu s$)

minimum values of dB/dt, determined by combining the minimum thresholds E_{min} in Table 1 with eqn. 5, in which the value $r = 0{\cdot}2$ m has been assumed. Table 3 also lists minimum thresholds in terms of the peak value of a rectangular stimulus field determined by

$$B_{min} = \tau(dB/dt)_{min} = \frac{2}{r}(\tau E_t)_{min} \quad (6)$$

where $(\tau E_t)_{min}$ has been obtained from Table 1. In eqn. 6, it is assumed that dB/dt is constant over τ, and that the flux density is zero at the begninning of the stimulus period. As suggested by Fig. 3, B_{min} applies to rectangular pulses of short duration ($\tau < 10\,\mu s$).

It is instructive to compare thresholds determined by the methods in this review with criteria established elsewhere. The National Radiological Protection Board (NRPB) of Great Britain has estimated thresholds for ventricular fibrillation at 3 $A m^{-2}$, and recommends a safety factor of 10 below that as the minimum permissible current density induced by MRI time-varying magnetic fields (NRPB, 1983). Including the safety factor, the NRPB magnetic field recommendation is 20 $T s^{-1}$ for exposure durations exceeding 10 ms; for $t < 10$ ms, allowed exposure may be increased in proportion to $t^{-1/2}$

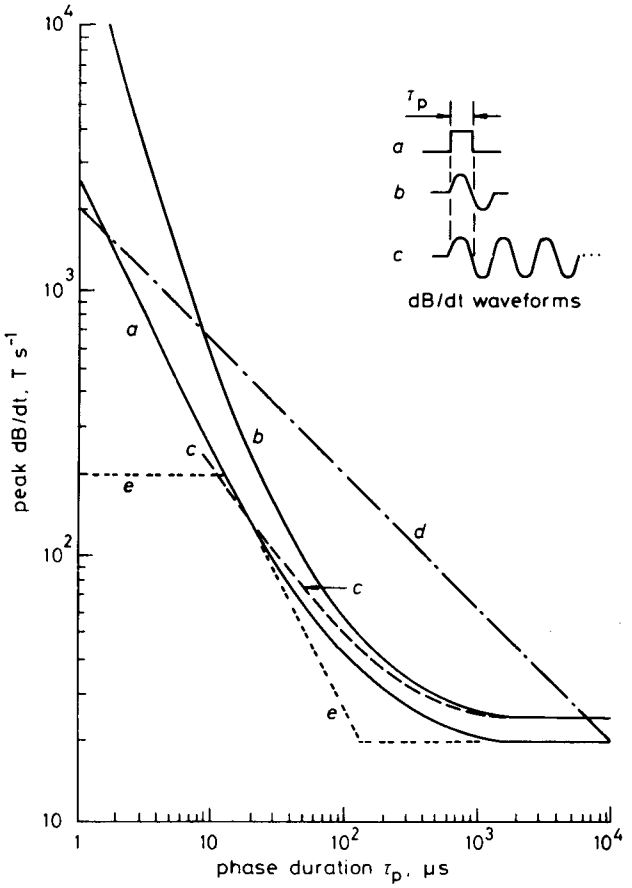

Fig. 9 *Thresholds for whole body exposure to time varying magnetic fields including safety factors (see text). Curves (a)–(c) based on SENN model. (a) rectangular dB/dt waveform; (b) single sinusoidal cycle; (c) continuous sinusoidal waveform; (d) NRPB guidelines; (e) simplified dB/dt acceptability criterion*

As a point of comparison, consider a minimum dB/dt threshold of 20 $T s^{-1}$ as suggested by the NRPB. This limit would imply safety factors of 3, 6 and 12 below the SENN model thresholds for 20, 10 and 5 μm fibres, respectively (Table 3). Curve (*a*) in Fig. 9 shows the strength/duration curve of Fig. 3, adjusted to achieve a minimum dB/dt value of 20 $T s^{-1}$. Curves (*b*) and (*c*) plot the corresponding thresholds for single-cycle and continuous sinusoidal stimulation, respectively. Threshold curves (*b*) and (*c*) have been scaled from curve (*a*) by applying scaling factors consistent with the relationships shown in Figs. 6 and 7. Curve (*d*) shows the NRPB criteria.

The rectangular pulse thresholds shown in Fig. 9 are below those for single-cycle sinusoidal stimulation at all values of the phase duration. The curve (*a*) thresholds are also below the continuous sinusoidal stimulation thresholds for phase durations above 10 μs (frequency below 50 kHz). The curve (*a*) values are also below the NRPB values for pulse durations above 1·5 μs.

Curve (*a*) thresholds may also be applied to repetitive pulses, as long as the repetition interval exceeds some minimum value. Fig. 5 indicates that if the repetition interval exceeds 500 μs, the excitation threshold for a pulse train is equivalent to that for a single pulse. For repetition intervals below 500 μs, curve (*a*) thresholds should be reduced in accordance with the multiplier shown in Fig. 5.

It might be inferred from Fig. 9 that dB/dt thresholds can be increased indefinitely as the phase duration is reduced. There is, however, a practical limit due to thermal perception from resistive heating. Experimental data on human perception of continuous sinusoidal currents show that thermal thresholds are lower than electrical stimulation thresholds for stimulus frequencies above 100 kHz (CHATTERJEE *et al.*, 1986), i.e. for $\tau_p < 5$ μs. By extrapolating curve (*c*) to $\tau_p = 5$ μs, the threshold value $dB/dt = 350$ $T s^{-1}$ is obtained. Note that this value would include in the thermal limit the same safety factor that is already included in the electrical thresholds of Fig. 9.

Curve (*e*) of Fig. 9 represents a simplified criterion for dB/dt; it is a straight-line approximation to curve (*a*) such that $dB/dt = 20$ $T s^{-1}$ for $\tau_p \geqslant 120$ μs, and increasing in proportion to τ_p^{-1} for $\tau_p < 120$ μs. A limiting value of 200 $T s^{-1}$ assures that the threshold established by curve (*c*) is not exceeded. This limit also provides an additional safety factor below the presumed thermal limit for continuous sinusoidal stimulation. For repetitive unidirectional pulses, the repetition period is assumed to be greater than 500 μs. Otherwise, thresholds established for curves (*a*) and (*c*) should be reduced as suggested by Fig. 5.

6 Discussion

The intent of this review has been to present a rational and consistent methodology with which to determine peripheral nerve stimulation thresholds for complex current waveforms. By using a neuroelectric model, it has been possible to define the excitation thresholds and interrelationships for a variety of stimulus waveform types, including monophasic and biphasic pulse sequences, as well as sinusoidal stimuli. The advantage of using the

model is that it unifies the analysis of diverse waveform types, such that relative thresholds can be determined in a rational and consistent manner. In addition, the model results agree quite well with a variety of data from human and animal experimentation.

The magnetic field exposure curves shown in Fig. 9 have been based on a number of conservative assumptions. These are:

(*a*) *Exposure area.* An exposure radius of 0·2 m has been adopted. This represents a rather extreme case that might apply only to whole-body exposure of a large person.
(*b*) *Spatial uniformity.* The peak magnetic field has been assumed to exist uniformly within the exposure area. This may represent a pessimistic assumption for some applications. With MRI exposure for example, the B-field is not uniform along all axes, and may undergo a phase change within a given spatial plane.
(*c*) *Nerve fibre size.* Thresholds have been analysed in terms of an extreme value (20 μm) within the distribution of neuron fibres present in the human body. Thresholds for smaller fibres are reduced in proportion to fibre size.
(*d*) *Safety factor.* The thresholds shown in Fig. 9 include a safety factor of 3 in addition to all of the other conservative factors enumerated above.

The stimulation thresholds addressed here are considered to be biologically significant endpoints for acceptability criteria. Even though the threshold reaction is expected to be functionally mild, the dynamic range for electrical stimulation is very small in comparison with natural excitation modalities. For example, with single-pulse electrocutaneous stimulation, a sensory change from perception to pain spans a range of about 3 or 5 to 1, depending on the site of stimulation (REILLY and LARKIN, 1984; 1987). Furthermore, if repetitively pulsed stimuli are individually at or above the excitation threshold, both sensory and muscular response can increase dramatically relative to that for a single pulse (REILLY and LARKIN, 1987).

The development of acceptability standards for magnetically induced currents should consider potential biological effects other than peripheral nerve stimulation. For example, time-varying magnetic fields applied to the head can create visual effects. Induction of phosphenes has been reported at a current density as low as 0.002 $A\,m^{-2}$ (BERNHARDT, 1985), a level 1000 times smaller than the peripheral stimulation thresholds reported in this review. Considering the low thresholds, and sharply defined sensitivity with respect to stimulus frequency, phosphene stimulation is quite unlike that for peripheral nerve excitation.

Cardiac excitation is another effect that needs to be taken into account when developing acceptability standards. A 30 per cent increase in the beating rate of isolated frog hearts has been reported for sinusoidal fields with a peak value as low as $5\,V\,m^{-1}$ at the most sensitive frequency (0·7 Hz) (KLOSS and CARSTENSEN, 1983). Ventricular fibrillation thresholds have been cited at field strengths as low as $8\,V\,m^{-1}$, leading to a current density of $2{\cdot}0\,A\,m^{-2}$ (BERNHARDT, 1985). Current density thresholds for ventricular fibrillation have been inferred from cardiac contact electrode data to be as low as $5.0\,A\,m^{-2}$ (ROY *et al.*, 1985). The National Radiological Protection Board of Great Britain has estimated thresholds for ventricular fibrillation at $3\,A\,m^{-2}$ (NRPB, 1983).

The ratios of experimental cardiac excitation thresholds to the minimum values are expressed in Table 1 for peripheral stimulation range from 0·8 to 4. In studies with rats (MCROBBIE and FOSTER, 1985), when pulsed fields exceeded the peripheral stimulation values expressed in items 1–3 of Table 2, cardiac abnormalities could not be produced, even at levels causing violent muscle contractions. The development of cardiac stimulation thresholds for complex waveform stimuli will need careful attention in future studies.

This review has emphasised whole-body exposure to time-varying magnetic fields. There are also clinical diagnostic applications where magnetic fields are applied locally via small coils to the brain or peripheral nervous system (BARKER *et al.*, 1987). The techniques employed in this review may also be applied to analyse local magnetic field stimulation, although it would require more rigorous attention to the spatial distribution of internal induced fields. It is possible that the spatial gradient of the electric field may be significant for small magnetic exposure systems. To evaluate the locus and threshold of stimulation would require an analysis that accounted for the distribution of induced voltage disturbances within the biological medium, and the size, orientation and terminal positions of the neurons.

Acknowledgments—The author gratefully acknowledges support and valuable technical interchange with members of the Center for Devices & Radiological Health of the US Food & Drug Administration. In particular thanks are extended to M. P. Anderson, T. W. Athey and P. Czerski.

References

ANDERSON, A. B. and MUNSON, W. A. (1951) Electrical stimulation of nerves in the skin at audio frequencies. *J. Acoust. Soc. Am.*, **23**, 155–9.

BARKER, A. T., FREESTON, I. L., JALINOUS, B. and JARRATT, J. A. (1987) Magnetic stimulation of the human brain and peripheral nervous system: an introduction and the results of an initial clinical evaluation. *Neurosurg.*, **20**, 100–109.

BERNHARDT, J. H. (1985) Evaluation of human exposures to low frequency fields. The impact of proposed frequency radiation standards on military operations. Lecture Series 138, Advisory Group for Aerospace Res. & Dev. (NATO), Surseine, France.

BRAZIER, M. A. (1977) *Electrical activity of the nervous system.* Williams & Williams Co., Baltimore.

CARUSO, P. M., PEARCE, J. A. and DEWITT, D. P. (1979) Temperature and current density distributions at electrosurgical dispersive electrode sites. Proc. 7th New England Bioeng. Conf., Troy, New York, 22nd–23rd March, 373–376.

CHATTERJEE, I., WU, D. and GANDHI, O. P. (1986) Human body impedance and threshold currents for perception and pain for contact hazard analysis in the VLF-MF band. *IEEE Trans.*, **BME-33**, 486–494.

DALZIEL, C. F. (1972) Electric shock hazard. *IEEE Spectrum*, **9**, (2), 41–50.

FRANKENHAEUSER, B. and HUXLEY, A. F. (1964) The action potential in the myelinated nerve fiber of *Xenopus laevis* as computed on the basis of voltage clamp data. *J. Physiol.*, **171**, 302–315.

HODGKIN, A. L. and HUXLEY, A. F. (1952) A quantitative description of membrane current and its application to conduction and excitation in nerve. *Ibid.*, **117**, 500–544.

IRWIN, D., RUSH, S., EVERMY, R., LEPESCHKIN, E., MONTGOMERY, D. B. and WEGGEL, R. J. (1970) Stimulation of cardiac muscle by a time-varying magnetic field. *IEEE Trans.*, **MAG-6**, 321–322.

KANDEL, E. R. and SCHWARTZ, J. B. (1981) *Principles of neural science.* Elsevier/North-Holland, New York.

KLOSS, D. A. and CARSTENSEN, E. L. (1983) Effects of ELF electric fields on the isolated frog heart. *IEEE Trans.*, **BME-30**, 347–348.

MCNEAL, D. R. (1976) Analysis of a model for excitation of

myelinated nerve. *Ibid.*, **BME-23,** 329–337.
McNEAL, D. R. and TEICHER, D. A. (1977) Effect of electrode placement on threshold and initial site of excitation of a myelinated nerve fiber. In *Functional electrical stimulation.* HAMBRECHT, T. F. and RESWICK, J. B. (Eds.), Marcel Decker Inc., New York.
McROBBIE, D. and FOSTER, M. A. (1984) Thresholds for biological effects of time-varying magnetic fields. *Clin. Phys. Physiol. Meas.*, **5,** 67–78.
McROBBIE, D. and FOSTER, M. A. (1985) Cardiac response to pulsed magnetic fields with regard to safety in NMR imaging. *Phys. in Med. & Biol.*, **30,** 695–702.
NRPB, National Radiological Protection Board (1983) Revised guidance on acceptable limits of exposure during nuclear magnetic resonance clinical imaging. *Br. J. Radiol.*, **56,** 974–977.
POLSON, M. J. R., BARKER, A. T. and GARDINER, S. (1982*a*) The effect of rapid rise-time magnetic fields on the ECG of the rat. *Clin. Phys. Physiol. Meas.*, **3,** 231–234.
POLSON, M. J. R., BARKER, A. T. and FREESTON, I. L. (1982*b*) Stimulation of nerve trunks with time-varying magnetic fields. *Med. & Biol. Eng. & Comput.*, **20,** 243–244.
RANCK, J. B. (1975) Which elements are excited in electrical stimulation of mammalian central nervous system: a review. *Brain Res.*, **98,** 417–440.
REILLY, J. P. and LARKIN, W. D. (1983) Electrocutaneous stimulation with high voltage capacitive discharges. *IEEE Trans.*, **BME-30,** 631–641.
REILLY, J. P. and LARKIN, W. D. (1984) Understanding transient electric shock. *Johns Hopkins APL Tech. Dig.*, **5,** 296–304.
REILLY, J. P., FREEMAN, V. T. and LARKIN, W. D. (1985) Sensory effects of transient electrical stimulation — evaluation with a neuroelectric model. *IEEE Trans.*, **BME-32,** 1001–1011.
REILLY, J. P. and BAUER, R. H. (1987) Application of a neuroelectric model to electrocutaneous sensory sensitivity: parameter variation study. *Ibid.*, **BME-34,** 752–754.
REILLY, J. P. and LARKIN, W. D. (1987) Human sensitivity to electric shock induced by power frequency electric fields. *Ibid.*, **EMC-29,** 221–232.
REILLY, J. P. (1988) Neuroelectric models for electrical stimulation studies. *Johns Hopkins APL Tech. Dig.*, **9,** (1), 44–59.
ROY, O. Z., MORTIMER, A. J., TROLLOPE, B. J. and VILLENEUVE, E. J. (1985) Electrical stimulation of the isolated rabbit heart by short duration transients. pp. 77–86 In *Electrical shock safety criteria,* BRIDGES, J. E., FORD, G. L., SHERMAN, I. A. and VAINBERG, M. (Eds.), Pergamon Press, New York.
RUCH, T. C., PATTON, H. D., WOODBURY, J. W. and TOWE, A. L. (1968) *Neurophysiology,* W. B. Saunders Co., Philadelphia.
SAUNDERS, F. A. (1974) Electrocutaneous displays. Proc. Conf. on Cutaneous Communication Systems and Devices, The Psychonomic Society, Austin, Texas, 20–26.
SILNY, J. (1986) The influence of threshold of the time-varying magnetic field in the human organism. In *Biological effects of static and extremely low frequency magnetic fields.* BERNHARDT, J. H. (Ed), MMV Medzin Verlag, München, 105–115.
UENO, S., HARADA, K, JI, C. and OOMURA, Y. (1984) Magnetic nerve stimulation without interlinkage between nerve and magnetic flux, *IEEE Trans.*, **MAG-20,** 1660–1662.

Appendix

Myelinated nerve excitation model

Fig. 10 illustrates an electrical model for a myelinated nerve as formulated by McNEAL (1976). The individual nodes are shown as circuit elements comprising a transmembrane capacitance C_m, transmembrane resistance R_m and a potential source E_r which represents the transmembrane resting potential. The voltages $V_{e,n}$ refer to the external nodal voltages that result from the stimulus current. In the general case, these voltages are computed from the electric field produced by the stimulus current flowing within the biological medium.

McNeal studied an 11-node array with one central node as nonlinear and all the others as linear. Excitation current was introduced via an electrode nearby the central nonlinear node. He defined excitation as occurring when the nonlinear node reached a peak depolarisation value of 80 mV. For the range of stimuli studied by McNeal, this arrangement was entirely satisfactory. However, for a more general range of stimulus parameters, some modifications are required.

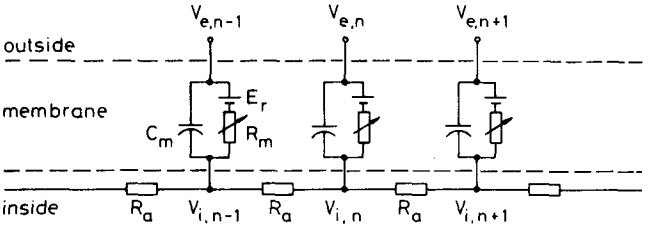

Fig. 10 *Equivalent circuit models for excitable membranes. The response near excitation threshold requires that the membrane conductance be described by a set of nonlinear differential equations*

The model used in this study is an extension of the one published by McNeal, with modifications to include FH nonlinearities at each of several adjacent nodes. Additional extensions include a test for excitation based on AP propagation,* the ability to model arbitrary stimulus waveforms, the representation of stimulation at the neuron terminus and the representation of stimulation by uniform electric fields. We refer to the extension of McNeal's model as the 'spatially extended nonlinear nodal' (SENN) model. Using the McNeal framework, the expression for transmembrane potential at the nth node is:

$$\frac{dV_n}{dt} = \frac{1}{C_m}[G_a(V_{i,n-1} - 2V_{i,n} + V_{i,n+1} + V_{e,n-1} - 2V_{e,n} + V_{e,n+1}) - \pi f d(i_{Na} + i_K + i_L + i_p)] \quad (7)$$

where C_m is the nodal capacitance, G_a is the nodal membrane conductance, V_n is the transmembrane voltage relative to the resting potential, $V_{e,n}$ is the external voltage at the nth node due to the stimulus current, $V_{i,n}$ is the internal voltage at the nth node, f is the fibre diameter and d is the nodal gap width. The terms i_{Na}, i_K, i_L and i_p are ionic currents whose magnitude and time response are related to membrane voltage through a set of nonlinear differential equations developed by FRANKENHAEUSER and HUXLEY (1964). Values for the various parameters in eqn. 7 and expressions for the ionic currents may be found in McNEAL (1976) and REILLY (1988). Using eqn. 7 for electrical stimulation applications, the $V_{e,n}$ values are known, and the V_n values are unknowns for which solutions must be found.

Before exercising the SENN model, it is generally necessary to first identify the approximate node where excitation is expected to begin. For this purpose, the system may be subjected to a subthreshold stimulus, while noting the voltage displacement at each node. The node responding with the greatest voltage displacement is the 'excitation node' where the threshold reaction may be expected to begin. It is necessary to surround the excitation node with an adequate number of 'nonlinear nodes' (those employing the full set of nonlinear FH equations) to ensure threshold accuracy, and to allow unambiguous determination of AP propagation. Additional nodes may use a linear description as indicated by Fig. 10 to conserve computer running time. As indicated by previous studies (REILLY *et al.*, 1985; REILLY and BAUER, 1987), a 21-node model with seven nonlinear nodes centred on the excitation node has proven satisfactory. The present study with uniform field excitation has extended the number of nonlinear nodes to 11 to provide a conservative margin of confidence in the results. Excitation is recognised on the basis of a propagating AP. The computer algorithm recognises this condition by testing for adequate depolarisation (80 mV) that propagates to the third node beyond the point of initial excitation. The threshold current value is determined by iterating between a current level causing excitation and a level not causing excitation. The iteration is continued until the

** The use of a single depolarisation voltage is not always an adequate indicator of excitation when brief oscillatory stimuli are used. In that case, a threshold test based on propagation is needed (REILLY et al., 1985).*

threshold and no-threshold levels differ by no more than 1 per cent. The resulting minimum excitation value is the SENN threshold.

To exercise the SENN model, it is necessary to specify along the axon the spatial distribution of voltage resulting from the stimulating current as well as the stimulus temporal pattern. In this review, magnetic induction thresholds were derived by assuming a distribution of voltages resulting from a uniform electric field:

$$V_{e,n} = V_{e,1} + EL(n-1) \tag{8}$$

where $V_{e,1}$ is a reference voltage at the terminal node, E is the electric field, L is the internodal space and n is the node number. For the SENN model L is chosen as 100 times the fibre diameter. In eqn. 8 it is assumed that the first node of the array is oriented toward the cathode of the current source. In the studies presented here, thresholds were found to be independent of $V_{e,1}$.

Table 4 presents electric field threshold values used in drawing

Table 4 SENN model electric field thresholds for uniform field excitation (10 μm fibre diameter)

τ_p, μs	E, V m^{-1}	$E\tau$, V s m^{-1}
2·5	595·3	1.49×10^{-3}
5	303·8	1.52×10^{-3}
10	158·4	1.58×10^{-3}
20	85·3	1.70×10^{-3}
50	41·0	2.05×10^{-3}
100	26·5	2.65×10^{-3}
200	18·6	3.73×10^{-3}
500	14·0	7.01×10^{-3}
1000	12·7	1.27×10^{-2}
2000	12·3	2.47×10^{-2}

Fig. 3. The values listed under the middle column represent SENN thresholds for the 10 μm fibre. The third column is simply the product of the first two columns. The minimum values $E = 12{\cdot}3$ V m^{-1} and $E\tau = 1.49 \times 10^{-3}$ V s m^{-1} have been used as normalising factors in Fig. 3. SENN thresholds were also obtained for 5 μm and 20 μm fibres excited by monophasic and biphasic pulses of several durations. Within the limits of the experimental error (1 per cent) SENN thresholds were found to be directly proportional to fibre diameter. Consequently, the normalised curves in Fig. 3 are equally valid for the other fibre sizes referred to in this review. The electric field normalisation factor $E = 12{\cdot}3$ V m^{-1} has also been used in Figs. 4 and 5, which also apply to uniform field excitation.

Elsewhere in this review (Figs. 6–8) threshold curves have been reproduced from a previous publication (REILLY *et al.*, 1985). For these curves, a 20 μm fibre was excited by a point electrode placed 2 mm from the central node of the array, with a passive electrode at a distant location. For this mode of stimulation the voltage disturbance at a distance r from the electrode is given by

$$V(r) = \rho I/(4\pi r) \tag{9}$$

where ρ is the resistivity of the medium. The excitation node for this method of stimulation will be at the node nearest the active point electrode if it is a cathode, and if the stimulus current is monophasic. If the active electrode is an anode, or if the stimulus is biphasic, the position of the excitation node may be at other locations (REILLY *et al.*, 1985).

As suggested by eqn. 9, the appropriate stimulus parameter is total current into the electrode, rather than the electric field, as suggested by eqn. 8 for uniform field excitation. Accordingly, Figs. 6 and 8 use units of current along the vertical axis. In Fig. 7, the normalising factors are the single cycle thresholds given in Fig. 6, at the corresponding frequencies. The normalised strength/duration data from Figs. 6–8 and the relative displacements of the curves have been used to construct curves (*b*) and (*c*) in Fig. 9.

A reasonable curve fit to the data in Table 4 is obtained from the expression derived for excitation of an ideal linear membrane: (REILLY and LARKIN, 1983)

$$E_t = E_{min}[1 - \exp(-\tau_p/\tau_e)]^{-1} \tag{10}$$

where E_t is the threshold electric field, E_{min} is the minimum threshold for long pulses and τ_e is an experimentally determined strength/duration time constant. In Table 4, $E_{min} = 12{\cdot}3$ V m^{-1}, and a least squares fit of the data to eqn. 10 yields $\tau_e = 120$ μs. Experimental values of τ_e have a range that includes 120 μs, although that value is near the low end of the experimental range (REILLY, 1988).

Author's biography

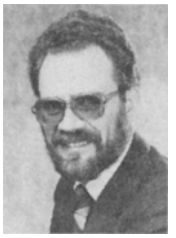

J. Patrick Reilly received the BEE degree from the University of Detroit in 1962, and the MSE from the George Washington University in 1966. He is a member of the Principal Professional Staff at the Johns Hopkins University Applied Physics Laboratory. He joined the Laboratory in 1962 and has worked there on radar and sonar, and electromagnetic and acoustic interactions with environmental and biological systems. He is now with the Fleet Systems Department, where he is responsible for radar system studies and bioelectric research activities. He is a senior member of the IEEE and is a member of the Bioelectromagnetics Society.